# Coevolution Maintains Diversity in the Stochastic "Kill the Winner" Model

Chi Xue and Nigel Goldenfeld*

*Department of Physics and Center for the Physics of Living Cells, University of Illinois at Urbana-Champaign, Loomis Laboratory of Physics, 1110 West Green Street, Urbana, Illinois 61801-3080, USA and Carl R. Woese Institute for Genomic Biology and Institute for Universal Biology, University of Illinois at Urbana-Champaign, 1206 West Gregory Drive, Urbana, Illinois 61801, USA*

(Received 8 June 2017; published 28 December 2017)

The "kill the winner" hypothesis is an attempt to address the problem of diversity in biology. It argues that host-specific predators control the population of each prey, preventing a winner from emerging and thus maintaining the coexistence of all species in the system. We develop a stochastic model for the kill the winner paradigm and show that the stable coexistence state of the deterministic kill the winner model is destroyed by demographic stochasticity, through a cascade of extinction events. We formulate an individual-level stochastic model in which predator-prey coevolution promotes the high diversity of the ecosystem by generating a persistent population flux of species.

DOI: 10.1103/PhysRevLett.119.268101

The high diversity of coexisting species in most ecosystems has been a major puzzle for more than 50 years. In a classic paper, Hutchinson articulated the so-called paradox of the plankton for the case of marine ecosystems [1,2]: Why do many species of plankton that feed on the same nutrients coexist, somehow avoiding the phenomenon of competitive exclusion [3], where one species outcompetes all the others?

The various tentative resolutions of the paradox can be divided into two classes [4–6]. In the first, the ecosystem is argued to have failed to reach a fixed point equilibrium state in which the competitive exclusion principle applies, due to temporal or/and spatial factors. For example, the time needed for the system to reach equilibrium might be much longer than the time over which the system undergoes significant changes in its boundary conditions, such as weather [7]. Spatial heterogeneity can increase the global diversity of the system by maintaining local patches that each obey the competitive exclusion principle but globally support the coexistence of multiple species [8,9] (for another perspective, see [10]). In the second class of resolutions, interactions such as predation, in conjunction with competitive exclusion, promote the coexistence of species through time-dependent or stochastic steady states [11–13]. One widely celebrated example of this behavior, which is seen in both natural ecosystems as well as some laboratory systems such as chemostats [14,15], is the continual succession of different community members known as "kill the winner" (KTW) dynamics [12,16]. This has been frequently revisited and expanded in the context of marine systems [17,18] and is related to the Janzen-Connell hypothesis [19,20] for tree biodiversity.

In the KTW hypothesis [12,16,17], there are two groups of resource consumers, for example, bacteria and plankton. The plankton community generally has a lower efficiency of resource usage than bacteria. They remain in the system, only because a protozoan consumes the bacteria nonselectively and thus limits the bacterial population, leaving room for plankton to thrive. Inside the bacterial community, different strains have distinct growth rates. They coexist, with no dominating winners, due to host-specific viruses controlling the corresponding strains. This results in two layers of coexistence through KTW dynamics (bacteria-plankton coexistence and bacterial strain coexistence), nested like Russian dolls [17].

The original KTW model [12,16] was formulated as deterministic Lotka-Volterra-type equations for the species biomass concentrations. The high diversity of the system is exhibited in the steady state where multiple species coexist with positive biomass; these calculations assume that the system is spatially homogeneous and that the number of individuals is large enough so that it is valid to use a continuous density to describe the population. However, this is not appropriate when the population is finite, because large fluctuations are able to drive the system towards extinction, an outcome that cannot be captured by a continuous density that is allowed to become arbitrarily small [21,22]. Requiring the population size to be integer-valued leads inexorably to shot noise, referred to in the ecological context as demographic stochasticity.

The purpose of this Letter is to explore the effect of demographic stochasticity on the KTW paradigm and demonstrate that the stochasticity causes the coexistence steady state in the deterministic KTW model to break down through a cascade of extinctions, leading to a loss of diversity. This cascade can be avoided by allowing the predators and prey to coevolve by mutation. We propose a stochastic model of the coevolution and show that it generically maintains the diversity of the ecosystem, even in the absence of spatial extension. Our results for KTW models complement earlier findings that mutation controls

 

the diversity of strategies in more abstract models of ecosystems, idealized as evolutionary games, such as the prisoner's dilemma [23]. Our results strongly suggest that diversity reflects the dynamical interplay between ecological and evolutionary processes and is driven by how far the system is from an equilibrium ecological state (as could be quantified by deviations from detailed balance). The surprisingly deep role of demographic stochasticity uncovered here is consistent with earlier demonstrations that individual-level minimal models capture a wide variety of ecological phenomena, including large-amplitude persistent population cycles [24], anomalous phase shifts due to the emergence of mutant subpopulations [25,26], spatial patterns [27,28], and even reversals of the direction of selection [29] without requiring overly detailed modeling of interspecies interactions.

*Model.*—The key component of the KTW hypothesis is that, for each resource competitor, there is a corresponding predator that can prevent it from becoming a dominant winner. The Russian-doll-like hierarchy is not essentially important for the basic idea. Thus, we focus on only a single layer of KTW interaction, the host-specific viral infection, and ignore the multilevel structure.

We write down the individual reactions for a simplified system of $m$ pairs of prey and predators, which we will take to be bacteria and viruses (phages), as follows:

$$X_i \xrightarrow{b_i} 2X_i, \qquad X_i + X_j \xrightarrow{e_{ij}} X_j, \tag{1a}$$

$$Y_i + X_i \xrightarrow{p_i} (\beta_i + 1)Y_i, \qquad Y_i \xrightarrow{d_i} \varnothing. \tag{1b}$$

All rates are positive. $i, j = 1, 2, \ldots, m$ are strain indices. Bacterial individuals $X_i$ have strain-specific growth rate $b_i$. They compete with each other for an implicit resource with strength $e_{ij}$. Viruses of the $i$th strain $Y_i$ infect the corresponding host $X_i$ with rate $p_i$ and burst size $\beta_i$ and decay to nothing $\varnothing$ with rate $d_i$. These reactions form the minimal generalized KTW model.

Below are the corresponding mean-field rate equations:

$$\dot{B}_i = b_i B_i - \sum_{j=1}^{m} e_{ij} B_i B_j - p_i B_i V_i, \tag{2a}$$

$$\dot{V}_i = \beta_i p_i B_i V_i - d_i V_i. \tag{2b}$$

The dot operator stands for the time derivative. $B_i$ and $V_i$ represent the densities of the $i$th bacterial and viral strains, respectively. The competition matrix $e_{ij}$ is sometimes taken as random [30] or, more realistically, as arising from evolutionary dynamics, such as in a food web [31]. The KTW model describes situations where diversity is maintained by predation, with a secondary contribution from the competition $e_{ij}$. Here, we are interested in the sensitivity of KTW to stochasticity, and the conclusions are not changed if we set $e_{ij}$ to a constant value $e$ for simplicity.

Equation (2) has a nonzero steady state as shown below:

$$B_i^* = \frac{d_i}{\beta_i p_i}, \qquad V_i^* = \frac{1}{p_i}\left(b_i - e\sum_{j=1}^{m} B_j^*\right). \tag{3}$$

We require all $B_i^*$ and $V_i^*$ to be positive, which limits the parameters to satisfy $b_i > e\sum_{j=1}^{m} d_j/\beta_j p_j$, $\forall\ i$. Linear stability analysis shows that the steady state Eq. (3) is exponentially stable, with all eigenvalues of the linear stability matrix having negative real parts, as long as the quantity $x_i \equiv \beta_i p_i^2 B_i^* V_i^* = d_i(b_i - e\sum_{j=1}^{m} d_j/\beta_j p_j)$ is distinct for each $i$. The steady state can be either a focus or a node, depending on whether the eigenvalues have nonzero imaginary parts or not. The parameters used in this Letter result in the steady state being a focus, but the conclusion also applies to the node case.

In Fig. 1, we show in the first row the time series of prey and predator densities obtained from a numerical evolution of Eq. (2) for $m = 10$ pairs of bacteria and phages. Species

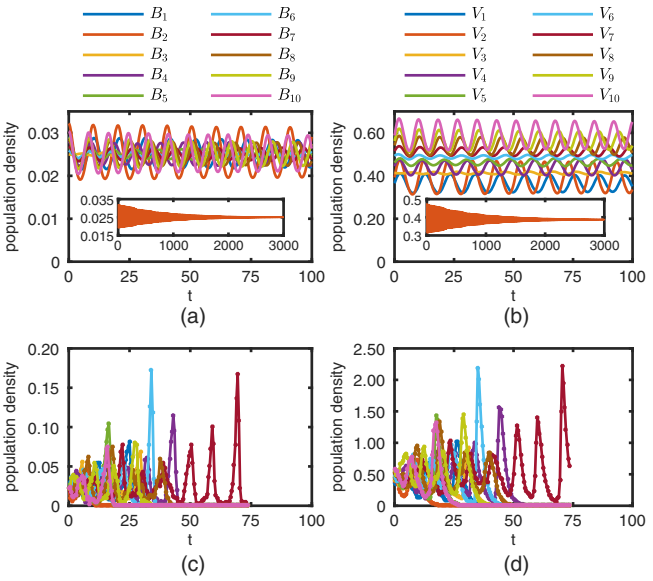


FIG. 1. Population density time series obtained from the generalized KTW framework, with ten bacterium-phage pairs. The left column is for bacteria and the right for viruses. The first row shows the result from a numerical evolution of the deterministic generalized KTW equations, with species densities initially perturbed randomly away from the steady state. The parameters are $\boldsymbol{b} = (0.75, 0.8, 0.85, 0.9, 0.95, 1, 1.05, 1.1, 1.15, 1.2)$, $p_i \equiv p = 2$, $\beta_i \equiv \beta = 10$, $d_i \equiv d = 0.5$, and $e_{ij} \equiv e = 0.1$. The insets show the long time behavior, which demonstrates that the steady state is a focus. For readability, only the decays of $B_2$ and $V_2$ are shown. The second row presents a typical simulation result of the stochastic version of the generalized KTW model, using the same set of parameters. The system size is $C = 1000$, and populations are initialized with the steady state value.

densities are initially perturbed away from the steady state. As shown in the figure insets, species densities decay back to the steady state at long times, confirming the result of the linear stability analysis. The oscillatory behavior at short time scales demonstrates the steady state to be a focus.

To reveal the effect of demographic noise, we also conduct the stochastic simulation of the corresponding individual level reactions (1) with the same parameter set, using the Gillespie algorithm [32]. The resultant species density time series are shown in the second row in Fig. 1. In contrast to the deterministic behavior of oscillatory decay, species go extinct in a short time. Bacterial strains become extinct due to a random fluctuation; this consequentially triggers the extinction of the corresponding viral strains, due to a lack of food. The number of species monotonically decreases in the process, and the system diversity undergoes a cascade.

The reason that the stable deterministic steady state of the generalized KTW model cannot be maintained in the presence of demographic stochasticity lies in the fact that species populations in the stochastic model are all finite, and the probability of the population reaching zero due to a random fluctuation is always nonzero.

Ecosystems have evolved many potential mechanisms to get around the path to extinction, as introduced at the beginning of the Letter. Here, we discuss one possibility: Prey and predator coevolve with each other so that fit mutants are constantly being introduced into the system, thus preventing the elimination of the species. Specifically, prey improve their phenotypic traits (e.g., strengthening the shell) to escape from predators, and predators also adjust their corresponding traits (e.g., sharpening the claws) to catch prey. This coevolutionary arms race has been well documented in many systems [33,34]. Previous theoretical studies focused on the dynamics of the traits of prey and predator groups [35–37], and the structure of the predation network [38], under different coevolving modes. Here, we study how coevolution affects the diversity of the host-specific predation system.

*Coevolution model.*—We modify the stochastic generalized KTW model (1) by adding in the following two sets of reactions to describe mutations of the prey $X_i$ from strain $i$ to $i \pm 1$, and similarly those of the predator $Y_i$:

$$X_i \xrightarrow{\mu_1/2} X_{i\pm1}, \qquad Y_i \xrightarrow{\mu_2/2} Y_{i\pm1}. \tag{4}$$

We assume that the mutation rates are strain independent and one individual can mutate into its two neighbor strains with the same rate, $\mu_1/2$ for bacteria or $\mu_2/2$ for viruses. We set the boundary condition to be open, so that mutations out of the index set $\{1, 2, \ldots, m\}$ are ignored. We will refer to Eqs. (1) and (4) as the coevolving KTW (CKTW) model.

For sufficiently high mutation rates, the absorbing extinction state in the generalized KTW model can be avoided, in the sense that a strain can reemerge as mutants are generated from its neighbor relatives after its population drops to zero. Therefore, mutation can stimulate a flux of population through different strains and promote coexistence.

We define the diversity of the system in the CKTW model using the Shannon entropy, $S = -\sum_{i=1}^{m} f_i \ln f_i$. Here, $f_i$ is the fraction of the $i$th bacterial (viral) strain in the entire bacterial (viral) community. The expression reaches the maximum, when all strains coexist at their deterministic steady state Eq. (3), and the minimum 0, when only one strain exists. We score $S = -1$ if either the bacterial or viral community goes extinct.

We present population density time series in Fig. 2 and the dependence of prey diversity on the mutation rates in Fig. 3. We set $\mu_1 = \mu_2 \equiv \mu$ for simplification. The diversity of the prey community is calculated at the end of the diversity time series shown in the inset in Fig. 3(a), after the system has gone through the transient region. Although, in principle, species in a stochastic system will always go extinct at a time exponentially long depending on the population size [22], this extinction time scale is not relevant in our simulation, and we thus focus on the system state in the long steady region before the destined collapse.

For a small enough mutation rate (population time series not shown), the entire community can become extinct before mutants can emerge, and the system still collapses, demonstrated by the diversity time series in the inset in Fig. 3(a), as in the generalized KTW model. This corresponds to region I in Fig. 3(a). For intermediate mutation rates, most strains stay near extinction, driven by

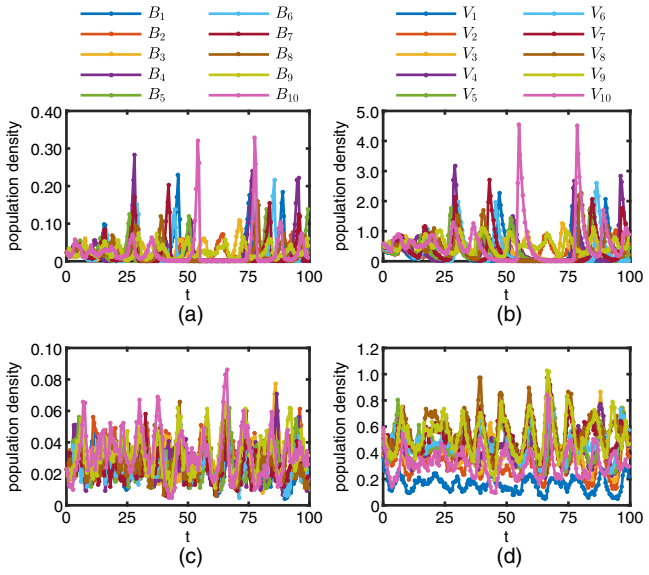


FIG. 2. Population density time series in the stochastic coevolving KTW model. The left column is for bacteria and the right for viruses. The system size is $C = 1000$, and the mutation rates are set to be equal, $\mu_1 = \mu_2 \equiv \mu$. Other rates are the same as those in Fig. 1. The upper and lower rows show the cases of low and high mutation rates, $\mu = 0.015$ and $\mu = 1$, respectively.

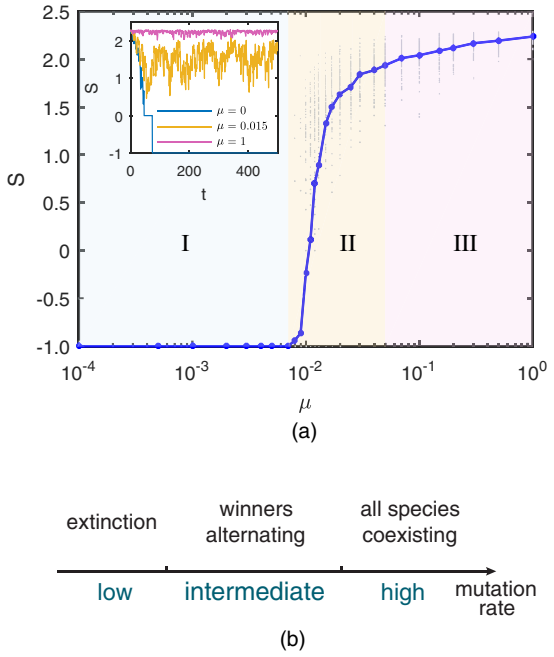


FIG. 3. (a) The main figure shows the prey diversity $S$, defined in the main text, as a function of the mutation rate $\mu_1 = \mu_2 \equiv \mu$. For each value of $\mu$, we conduct 100 replicates and calculate the diversity values at the end of the simulations, represented by the gray dots with the blue one being their mean. The inset shows diversity time series at mutation rates from the three regions, with $\mu = 0$, 0.015, and 1, respectively. For this particular set of parameters, the mean-field generalized KTW equations give an equal bacterial strain concentration at the steady state, and the maximum diversity in the corresponding CKTW model is $\ln m$. (b) A descriptive phase diagram of the dynamics, with the mutation rate as the tuning parameter.

demographic noise, while some mutants can grow to be dominant if they happen to confront only a few predators when first emerging. Subsequently, the predator population expands, feeding on the dominating winners, thus reducing the winner population, and allowing the next dominator to grow. In this way, we see that winner populations spike alternatively in the time series, as in the first row in Fig. 2. Near the onset of coexistence, the diversity has a large deviation and is very sensitive to the mutation rate, as shown in region II in Fig. 3(a). The large deviation is also seen in the diversity time series in the inset. For a large mutation rate, the coevolution-driven population flow is fast enough to compensate for the demographic fluctuations. All strains remain near the steady state, and no one can win over others, as shown by the population time series in the second row in Fig. 2. The diversity slowly approaches the maximum, with small deviations, as demonstrated in region III in Fig. 3(a). For an extremely large mutation rate (figures not shown), we cannot view the mutation as a perturbation to the ecological population dynamics. Species populations deviate from the mean-field steady state Eq. (3). Specifically, under the boundary condition in our model, in which the mutations out of the species space $\{1, 2, \ldots, m\}$ are effectively individual death, the population leaks through the boundary and eventually reaches zeros at extremely large mutation rates. According to the above discussion, we show three phases of dynamics, as illustrated in Fig. 3(b): the extinction phase at a low mutation rate, the winner-alternating phase at an intermediate mutation rate, and the coexisting phase at a high mutation rate.

*Open system model.*—So far, we have preassigned a fixed number of predator-prey pairs in the system. A more realistic approach is to let the system be open and evolve by itself to establish however many species there can be.

As mutants take on new traits, the population spreads in the trait space. This expansion usually is associated with a trade-off in the fitness [35]: The further the trait is from the origin, the lower the growth rate becomes. We model this trade-off effect, assuming a 1D trait space, by setting up $M$ species and assigning the highest birth rate to the species with index $M/2$, and decreasing the birth rate as the species index goes from $M/2$ to 1 and from $M/2$ to $M$. The species with index $M/2$ is at the center of the trait space and then is the origin of the trait expansion. Species 1 and $M$ have the lowest birth rates that are almost 0, and further mutation of the two will result in mutants with negative birth rates, which cannot grow and are thus excluded from the model. The species space $\{1, 2, \ldots, M\}$ contains all possible species that can potentially exist in the system. However, under conditions of resource limitation, formulated by the competition strength $e$, only a few with relatively high growth rates, out of $M$, can eventually be established in the system. The number of species that manage to thrive corresponds to $m$ in the previous models.

See Supplemental Material [39] for the stochastic simulation parameters and the resultant population time series and diversity dependence on the mutation rate. Even though the number of established pairs varies with time and the population leaks out of the region deterministically allowed by the carrying capacity, the system still exhibits three phases depending on the mutation rate, similar to the CKTW model with a fixed number of species.

*Discussion.*—In contrast to the model in Ref. [18], where killing winners is exerted externally, we focus on the intrinsically established KTW of the system. In the intermediate and fast mutation regions of the CKTW model, the ecological and evolutionary dynamics are coupled to each other and occur on the same time scale. This type of coupling can most easily be observed in microbial systems, in which organisms have a high mutation frequency [26,40,41]. Recent work has shown clearly the existence of genomic islands, where genomes of different strains vary in loci thought to be associated with phage resistance [42]. Both host-specific predation and mutation are important in generating the observed diversity of the bacterial genome. The minimal CKTW model can, in principle, describe the

diversity in the above system. For example, by controlling the mutation rate through an inducible promoter, using molecular techniques pioneered in Ref. [43], we envisage a fast bacterium-phage coevolution experiment to test the predicted phase diagram.

In addition to inevitable simplification of biological details, both the generalized KTW and the coevolving KTW models assume that the system is well mixed, ignoring any spatial dispersion. Consequently, they cannot capture the reservoir effect [44] present in an ecosystem, which means that, for any local community, organisms in its surrounding environment can move into it, keeping it supplied and refreshed. Specifically, even if a species goes extinct in a local community, it can be reseeded there by the surrounding reservoir. Well-mixed models should be thought of as describing not the entire system but a much smaller correlation volume, in which local demographic stochasticity can be significant [27,45].

This work was supported by the National Aeronautics and Space Administration Astrobiology Institute (NAI) under Cooperative Agreement No. NNA13AA91A issued through the Science Mission Directorate. C. X. was partially supported by the L. S. Edelheit Family Biological Physics Fellowship from the Department of Physics, University of Illinois at Urbana-Champaign. We would like to thank Tron Frede Thingstad, Selina Våge, Hong-Yan Shih and Brendan Bohannan for helpful discussions.

*nigel@uiuc.edu

[1] G. E. Hutchinson, Am. Nat. **95**, 137 (1961).
[2] J. S. Clark, M. Dietze, S. Chakraborty, P. K. Agarwal, I. Ibanez, S. LaDeau, and M. Wolosin, Ecol. Lett. **10**, 647 (2007).
[3] G. Hardin, Science **131**, 1292 (1960).
[4] J. B. Wilson, N. Z. J. Ecol. **13**, 17 (1990).
[5] S. Roy and J. Chattopadhyay, Ecol. Complex. **4**, 26 (2007).
[6] P. Chesson, Annu. Rev. Ecol. Syst. **31**, 343 (2000).
[7] R. Levins, Am. Nat. **114**, 765 (1979).
[8] P. Richerson, R. Armstrong, and C. R. Goldman, Proc. Natl. Acad. Sci. U.S.A. **67**, 1710 (1970).
[9] S. A. Levin, Am. Nat. **108**, 207 (1974).
[10] J. W. Fox, Trends Ecol. Evol. **28**, 86 (2013).
[11] M. Scheffer, S. Rinaldi, J. Huisman, and F. J. Weissing, Hydrobiologia **491**, 9 (2003).
[12] T. Thingstad and R. Lignell, Aquatic Microbial Ecology **13**, 19 (1997).
[13] K. Vetsigian, R. Jajoo, and R. Kishony, PLoS Biol. **9**, e1001184 (2011).
[14] A. Fernández, S. Huang, S. Seston, J. Xing, R. Hickey, C. Criddle, and J. Tiedje, Appl. Environ. Microbiol. **65**, 3697 (1999).
[15] S. Louca and M. Doebeli, Environ. Microbiol. **19**, 3863 (2017).
[16] T. F. Thingstad, Limnol. Oceanogr. **45**, 1320 (2000).
[17] C. Winter, T. Bouvier, M. G. Weinbauer, and T. F. Thingstad, Microbiol. Mol. Biol. Rev. **74**, 42 (2010).
[18] S. Maslov and K. Sneppen, Sci. Rep. **7**, 39642 (2017).
[19] D. H. Janzen, Am. Nat. **104**, 501 (1970).
[20] J. H. Connell, in *Dynamics of Population*, edited by P. J. den Boer and G. R. Gradwell (PUDOC, Wageningen, The Netherlands, 1971), pp. 298–312.
[21] O. Ovaskainen and B. Meerson, Trends Ecol. Evol. **25**, 643 (2010).
[22] O. Gottesman and B. Meerson, Phys. Rev. E **85**, 021140 (2012).
[23] D. F. Toupo, D. G. Rand, and S. H. Strogatz, Int. J. Bifurcation Chaos Appl. Sci. Eng. **24**, 1430035 (2014).
[24] A. J. McKane and T. J. Newman, Phys. Rev. Lett. **94**, 218102 (2005).
[25] T. Yoshida, L. E. Jones, S. P. Ellner, G. F. Fussmann, and N. G. Hairston, Nature (London) **424**, 303 (2003).
[26] H.-Y. Shih and N. Goldenfeld, Phys. Rev. E **90**, 050702 (2014).
[27] U. C. Täuber, J. Phys. A **45**, 405002 (2012).
[28] T. Butler and N. Goldenfeld, Phys. Rev. E **80**, 030902 (2009).
[29] G. W. A. Constable, T. Rogers, A. J. McKane, and C. E. Tarnita, Proc. Natl. Acad. Sci. U.S.A. **113**, E4745 (2016).
[30] R. M. May, Nature (London) **238**, 413 (1972).
[31] A. J. McKane, Eur. Phys. J. B **38**, 287 (2004).
[32] D. T. Gillespie, J. Comput. Phys. **22**, 403 (1976).
[33] S. T. Chisholm, G. Coaker, B. Day, and B. J. Staskawicz, Cell **124**, 803 (2006).
[34] A. Buckling and P. B. Rainey, Proc. R. Soc. B **269**, 931 (2002).
[35] U. Dieckmann, P. Marrow, and R. Law, J. Theor. Biol. **176**, 91 (1995).
[36] A. Agrawal and C. M. Lively, Evol. Ecol. Res. **4**, 91 (2002).
[37] J. S. Weitz, H. Hartman, and S. A. Levin, Proc. Natl. Acad. Sci. U.S.A. **102**, 9535 (2005).
[38] S. J. Beckett and H. T. Williams, Interface Focus **3**, 20130033 (2013).
[39] See Supplemental Material at http://link.aps.org/supplemental/10.1103/PhysRevLett.119.268101 for simulations of an open coevolving ecosystem. It provides detailed stochastic simulation parameters, and the resultant population time series and diversity dependence on the mutation rate.
[40] B. J. Bohannan and R. E. Lenski, Ecology **78**, 2303 (1997).
[41] T. Yoshida, S. P. Ellner, L. E. Jones, B. J. Bohannan, R. E. Lenski, and N. G. Hairston, Jr., PLoS Biol. **5**, e235 (2007).
[42] F. Rodriguez-Valera, A.-B. Martin-Cuadrado, B. Rodriguez-Brito, L. Pašić, T. F. Thingstad, F. Rohwer, and A. Mira, Nat. Rev. Microbiol. **7**, 828 (2009).
[43] N. H. Kim, G. Lee, N. A. Sherer, K. M. Martini, N. Goldenfeld, and T. E. Kuhlman, Proc. Natl. Acad. Sci. U.S.A. **113**, 7278 (2016).
[44] A. Shmida and S. Ellner, Vegetatio **58**, 29 (1984).
[45] T. Butler and N. Goldenfeld, Phys. Rev. E **84**, 011112 (2011).

# Coevolution Maintains Diversity in the Stochastic "Kill the Winner" Model
## Supplemental Material

This Supplemental Material describes simulations of an open coevolving ecosystem, as described briefly in the main text. We construct a species space to manifest the trade-off in the birth rate due to mutation. For the particular set of parameters used in the simulations, there are $M = 20$ distinct pairs of preys and predators that can potentially exist in the system. The birth rates are $\boldsymbol{b} = (0.05, 0.15, 0.25, 0.35, 0.45, 0.55, 0.65, 0.75, 0.85, 0.95, 1, 0.9, 0.8, 0.7, 0.6, 0.5, 0.4, 0.3, 0.2, 0.1)$. The 11th species has the highest birth rate and is the origin of trait expansion. Mutations of the first and last species generating mutants with negative birth rates are excluded from the model. Other parameters are $p_i \equiv p = 2$, $\beta_i \equiv \beta = 10$, $d_i \equiv d = 0.5$, and $e_{ij} \equiv e = 1$. The individual level reactions have the same form as Eq. (1) and (4) in the main text, with index $i = 1, 2, \ldots, M$. In the mean-field situation, the carrying capacity allows the coexistence of 13 pairs, with indices from 5 to 17, while the rest 7 species are forbidden. In the presence of demographic stochasticity, mutants can emerge in the forbidden region in the species space, although they can not develop a significant population size, limited by the high competition with other individuals. The number of coexisting pairs can be greater that the value 13 predicted by the mean-field calculation, and varies with time. As shown in the prey population time series in Fig. S1(a) and (b), a small mutation rate results in the alternation of dominating winners, and a large mutation rate generates coexistence with much smaller fluctuations. Figure S1 (c) and (d) show the distribution of prey population across all species as a function of the distance to the winner, defined as the most abundant strain. The red bar graph stands for a snapshot at a certain moment, and the blue one represents the average of the distribution over a long time interval. It's clear that a winner stands out at low mutation rate, while no one is significantly dominant at high mutation rate. Figure S1(e) shows the dependence of prey diversity, defined as the Shannon entropy, on the mutation rate. The three regions as seen in the CKtW model with fixed number of pairs in the main text are recovered.

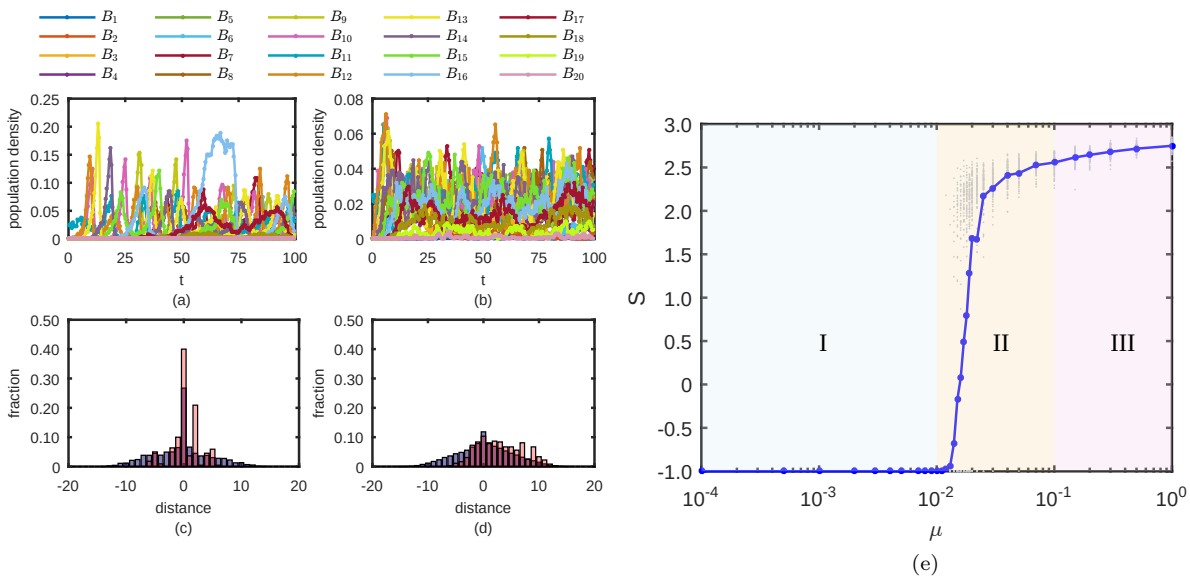


FIG. S1. Simulation results of the CKtW model with the number of coexisting species limited by the carrying capacity. Parameters used are $\boldsymbol{b} = (0.05, 0.15, 0.25, 0.35, 0.45, 0.55, 0.65, 0.75, 0.85, 0.95, 1, 0.9, 0.8, 0.7, 0.6, 0.5, 0.4, 0.3, 0.2, 0.1)$, $p_i \equiv p = 2$, $\beta_i \equiv \beta = 10$, $d_i \equiv d = 0.5$, and $e_{ij} \equiv e = 1$. The system size is $C = 1000$. Population is initiated in the fittest species and expands in the species space. (a) and (b) are prey population time series for small mutation rate $\mu_1 = \mu_2 \equiv \mu = 0.02$ and large mutation rate $\mu_1 = \mu_2 \equiv \mu = 0.5$, respectively. At small mutation rate, winners alternate with time and the population is localized to the winner species. At large mutation rate, all species coexist and the population distribution is roughly uniform in the mean-field allowed region, with some mutants leaked into the forbidden species. (c) and (d) show the prey population distribution across the species as a function of index distance from the winner strain, constructed from (a) and (b), respectively. The red bar graph is calculated at $t = 499.5$, after the transient regime. The blue one is the distribution averaged over 501 snapshots uniformly sampled between $t = 249.5$ and $t = 499.5$. For reference, the mean-field steady state predicts that species with indices from 5 to 17 coexist with equal abundance and that other species have zero population. The center bar at 0 distance is the population fraction of the most abundant strain. It's clear that a winner dominates at low mutation rate but not at the high one. (e) The dependence of prey Shannon entropy on the mutation rate, defined in the same way as in the main text. At low mutation, the system collapses due to extinction; at intermediate mutation, diversity increases rapidly with the rate; at high mutation, diversity stays near the maximum given by the deterministic steady state.